JOURNAL OF MATERIALS SCIENCE 30 (1995) 4003–4008

Oxides formed between ZrO_2 and Nb_2O_5

F. WANG, D. O. NORTHWOOD
Engineering Materials Group, Department of Mechanical Engineering, University of Windsor, Windsor, Ontario, Canada, N9B 3P4

High-purity monoclinic ZrO_2 and monoclinic Nb_2O_5 powder samples were mixed in varying ratios, and heated at 1300 °C for 24 h before furnace cooling. X-ray diffraction analysis showed that two compounds, $Nb_2O_5 \cdot 6ZrO_2$ and $Nb_2O_5 \cdot 8ZrO_2$ (or $(Zr, Nb)_8O_{17}$ and $(Zr, Nb)_{10}O_{21}$), were formed. Some of the reflections from the two compounds were overlapped and interfered with those from the zirconium oxide, especially the tetragonal ZrO_2. A thermodynamic analysis was used to demonstrate that it is possible to have ZrO_2 as well as Nb_2O_5 formed on Zr–Nb alloys in an oxidizing environment. The relevance of these results (experimental and calculated) to the corrosion of a Zr–Nb alloy in high temperature aqueous environments is discussed. It is suggested that the incorporation of niobium into the oxide during the corrosion of Zr–Nb alloys could be by the formation of compounds such as $(Zr, Nb)_8O_{17}$ and $(Zr, Nb)_{10}O_{21}$. Also, the tetragonal ZrO_2, which has been found to be a barrier layer oxide, could, in fact, be either of the ternary compounds $Nb_2O_5 \cdot 6ZrO_2$ and $Nb_2O_5 \cdot 8ZrO_2$ both of which are orthorhombic with lattice parameters very close to those of the tetragonal ZrO_2.

1. Introduction

A Zr–2.5 wt % Nb alloy is the material currently used in the manufacture of the pressure tubes for Canadian Deuterium Uranium Pressurized Heavy Water (CANDU–PHW) nuclear reactors. The Zr–2.5 wt % Nb alloy has replaced Zircaloy-2 as the current pressure tube material because of (i) its increased strength, allowing thinner-walled pressure tubing to be used, and hence a better neutron economy; and (ii) its better creep resistance [1]. As the alloy is currently used in the cold-worked condition, where it has a two-phase structure consisting of h c p α-Zr and b c c β-Zr [2, 3], so the oxide formed on the Zr–2.5 wt % Nb during aqueous corrosion (such as in-reactor) may incorporate elements such as niobium into the oxide, particularly if the oxide is formed on the high niobium-content β-phase of the two-phase (α + β) material: Fig. 1 shows the Zr–Nb binary phase diagram. However, little is known regarding the composition and structure of these oxides.

The most recent Nb–O–Zr ternary phase diagram shows no ternary intermediate compounds to be formed above 1000 °C [4], see Fig. 2. According to this phase diagram, and if we consider the simplified scheme of a straight line which runs between the Zr–2.5 Nb point and the oxygen corner as the diffusional path, then the oxide layer which forms on the metal as oxidation proceeds can be expected to have various structures, such as $(ZrO_2 + NbO)$ and $(ZrO_2 + NbO_2)$ and $(ZrO_2 + \beta(Nb))$ depending on its "position" with respect to the oxide–metal interface and the "free" oxide surface. Because there are no binary diagrams existing for either $(ZrO_2 + NbO_2)$ or $(ZrO_2 + NbO)$, and because both NbO_2 and NbO will transform to a more stable form, Nb_2O_5 under oxidizing conditions, it was considered useful to examine which compounds, if any, are formed between ZrO_2 and Nb_2O_5.

Several studies [5, 6] of the ZrO_2–Nb_2O_5 system have indicated the existence of considerable solid solubility of Nb_2O_5 in ZrO_2. A subsequent, more detailed, examination of this region of the phase diagram led to the identification of a new orthorhombic phase, with the composition of about $Nb_2O_5 \cdot 6ZrO_2$ [5], as can be seen in Fig. 3. Recently this phase has been shown to have a superstructure, which varies with compositions over a range from about $Nb_2O_5 \cdot 5ZrO_2$ to $Nb_2O_5 \cdot 8ZrO_2$ [7]. Fig. 4 differs from the corresponding region of Fig. 3 mainly in showing a narrower field

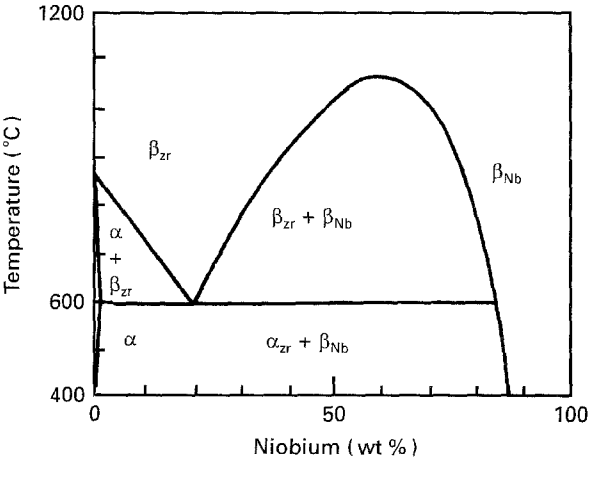

Figure 1 The zirconium–niobium equilibrium phase diagram.

0022–2461

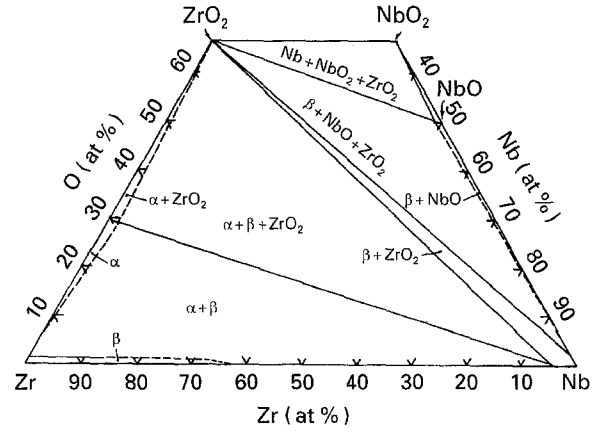

Figure 2 The Zr–Nb–O phase diagram above 1000 °C (assessed) [4].

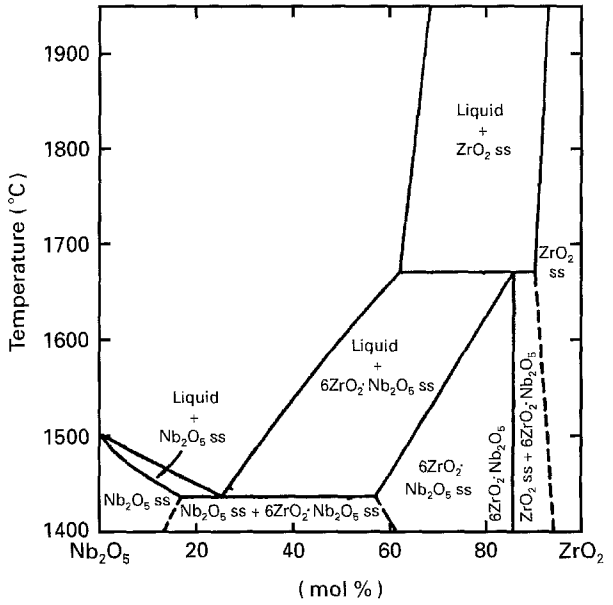

Figure 3 The ZrO_2–Nb_2O_5 system: ss = solid solution [5].

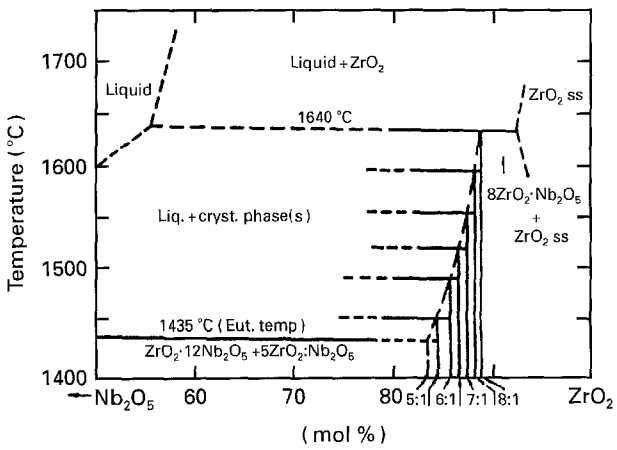

Figure 4 The proposed ZrO_2-rich portion of the Nb_2O_5–ZrO_2 system [7].

for the orthorhombic phase and in locating the composition of maximum stability at $Nb_2O_5 \cdot 8ZrO_2$ rather than $Nb_2O_5 \cdot 6ZrO_2$. These compositions of the superstructure were reported to belong to a continuous homologous series $[(Nb, Zr)_nO_{2n+1}]$ where n varies from ~7–10. The ZrO_2 solid solution region (in Fig. 4) was not studied and is taken from Fig. 3.

The results of an experimental examination of the compounds (if any) formed between ZrO_2 and Nb_2O_5 form the first part of this paper. In the second part, a thermodynamic analysis is used to demonstrate that it is possible to have ZrO_2 as well as Nb_2O_5 formed on Zr–Nb alloys in an oxidizing environment. The relevance of these results (experimental and calculated) to the corrosion of a Zr–Nb alloy is discussed.

2. Experimental procedure

High-purity ZrO_2 (>99%) and Nb_2O_5 (>99.9%) powder samples were mixed in varying ratios, with the mole fraction of Nb_2O_5 ranging from 20%–0.2%, see Table I. The ZrO_2 powder had a monoclinic structure, with lattice parameters $a = 0.531\,29$ nm, $b = 0.521\,25$ nm and $c = 0.514\,71$ nm. The Nb_2O_5 is also monoclinic, with $a = 2.0381$ nm, $b = 0.382\,49$ nm and $c = 1.9368$ nm. Both are odourless white powders.

A sample of each group was put into graphite crucibles and heated at 1300 °C for 24 h before furnace cooling to room temperature. The structure formed in the mixed oxides was determined by X-ray powder diffraction analysis. A Rigaku diffractometer using NaI (Tl) scintillator was used with graphite monochromated CuK_α radiation. The X-ray generator, goniometer and the counting system are computer controlled. A scanning speed of 2° min^{-1} in 2θ was used.

X-ray results showed that two new compounds, $Nb_2O_5 \cdot 6ZrO_2$ and $Nb_2O_5 \cdot 8ZrO_2$ were formed for all the samples tested. For example, Table II summarizes the X-ray diffraction analysis results of the oxides for the sample with 5% Nb_2O_5. The intensity of each reflection is indicated in brackets. Fig. 5 is the related X-ray diffraction pattern. It is important to note that some monoclinic ZrO_2 powder transformed to tetragonal ZrO_2. Fig. 6 shows the X-ray diffraction patterns of samples with 1%, 5% and 10% Nb_2O_5 as well as monoclinic ZrO_2. It is concluded from an examination of Figs 5 and 6 that (i) with a decrease in the amount of Nb_2O_5 in the samples, the intensities of the reflections from $Nb_2O_5 \cdot 6ZrO_2$ and $Nb_2O_5 \cdot 8ZrO_2$ decreased, indicating a smaller amount formed, and (ii) some of the diffraction peaks of these two compounds overlap and interfere with those of both monoclinic and tetragonal ZrO_2 powder. However, by looking for certain reflections that are isolated from the ZrO_2 reflections, i.e. at 2θ ~ 27.2°, 43.3°, 61.2° and 67.35° in Fig. 5, some of the $Nb_2O_5 \cdot 6ZrO_2$ and

TABLE I Chemical compositions of mixed oxides of ZrO_2 and Nb_2O_5

	Sample					
	1	2	3	4	5	6
ZrO_2 (%)	80	90	95	97.5	99	99.8
Nb_2O_5 (%)	20	10	5	2.5	1	0.2

TABLE II Comparison of the X-ray spectra for a sample of Nb_2O_5:ZrO_2 = 5:95 with the *d*-spacings of ZrO_2 (tetragonal), ZrO_2 (monoclinic), $Nb_2O_5 \cdot 6ZrO_2$ and $Nb_2O_5 \cdot 8ZrO_2$

Unknown (I)	ZrO_2 (T)	ZrO_2 (M)	$Nb_2O_5 \cdot 6ZrO_2$	$Nb_2O_5 \cdot 8ZrO_2$
3.695 (13)		3.690		
3.630 (16)		3.630		3.630
3.162 (70)		3.157		3.150
2.957 (100)	2.960		2.950	2.959
2.837 (50)		2.834		
2.639 (12)	2.635		2.640	2.640
2.601 (10)	2.600			
2.556 (9)			2.560	2.561
2.536 (8)	2.540	2.538		
2.496 (6)				2.493
2.211 (8)		2.213		
2.088 (4)			2.091	2.088
1.846 (10)		1.845		
1.835 (12)	1.830		1.838	1.839
1.814 (17)	1.810		1.809	1.812
1.783 (12)		1.780	1.782	1.785
1.577 (9)	1.575		1.579	1.579
1.541 (13)	1.547	1.541	1.545	1.543
1.515 (5)			1.511	1.514
1.509 (7)		1.508		
1.475 (9)		1.476	1.478	1.479
1.391 (2)			1.393	
1.321 (3)		1.321	1.321	
1.243 (1)			1.243	1.243
1.206 (1)	1.204		1.207	1.207
1.160 (4)	1.161		1.160	

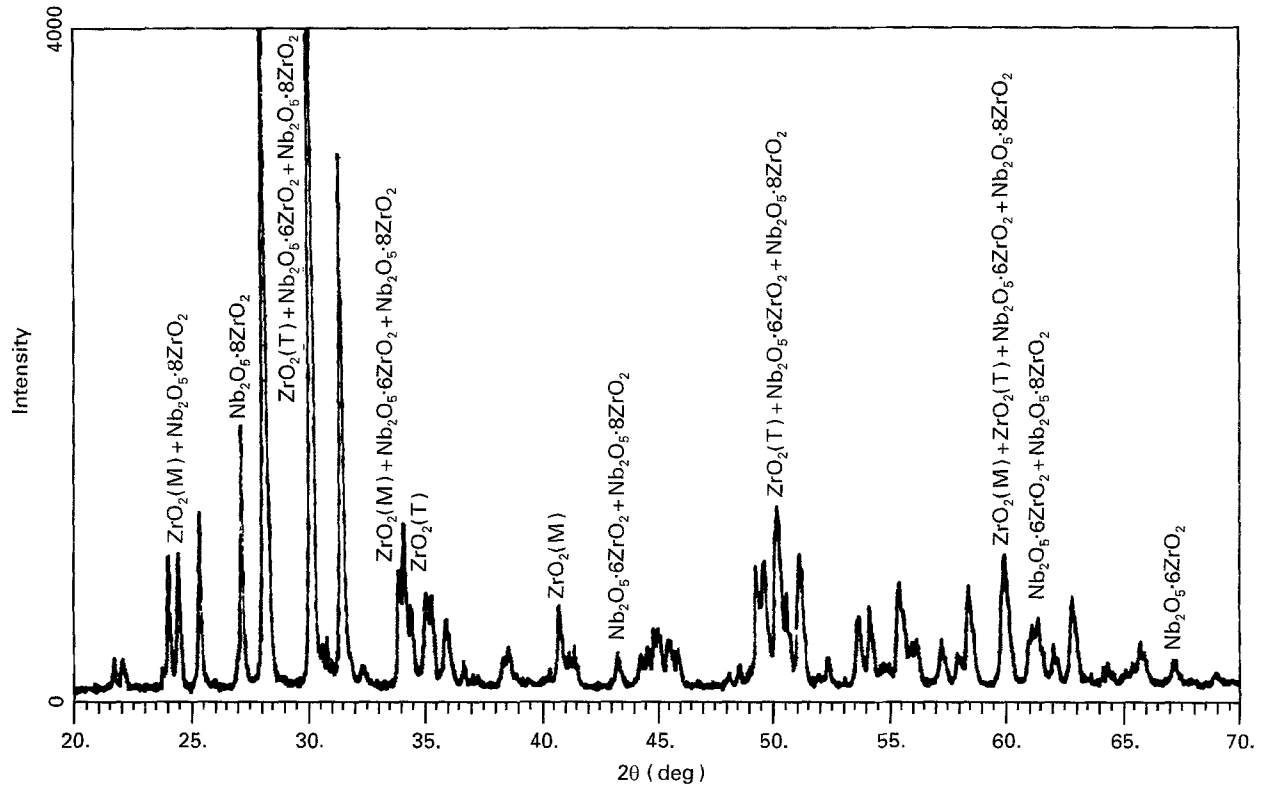

Figure 5 X-ray diffraction pattern of a sample with the molal fraction of Nb_2O_5:ZrO_2 = 5:95.

$Nb_2O_5 \cdot 8ZrO_2$ reflections could be positively identified.

3. Discussion

As mentioned in Section 1, most of the ternary data for the Zr–Nb–O system have been reported in the temperature range 1000–1600 °C. β-Zr and β-Nb form a complete series of solid solutions in this temperature range [4]. In the following calculations, we demonstrate on theoretical grounds that during the corrosion of Zr–Nb alloys in 300 °C water at 8.6 MPa (i.e. CANDU reactor conditions), both Nb_2O_5 and ZrO_2 could be formed.

First, it is necessary to calculate the Gibbs free energy of ZrO_2 and Nb_2O_5 formation under the

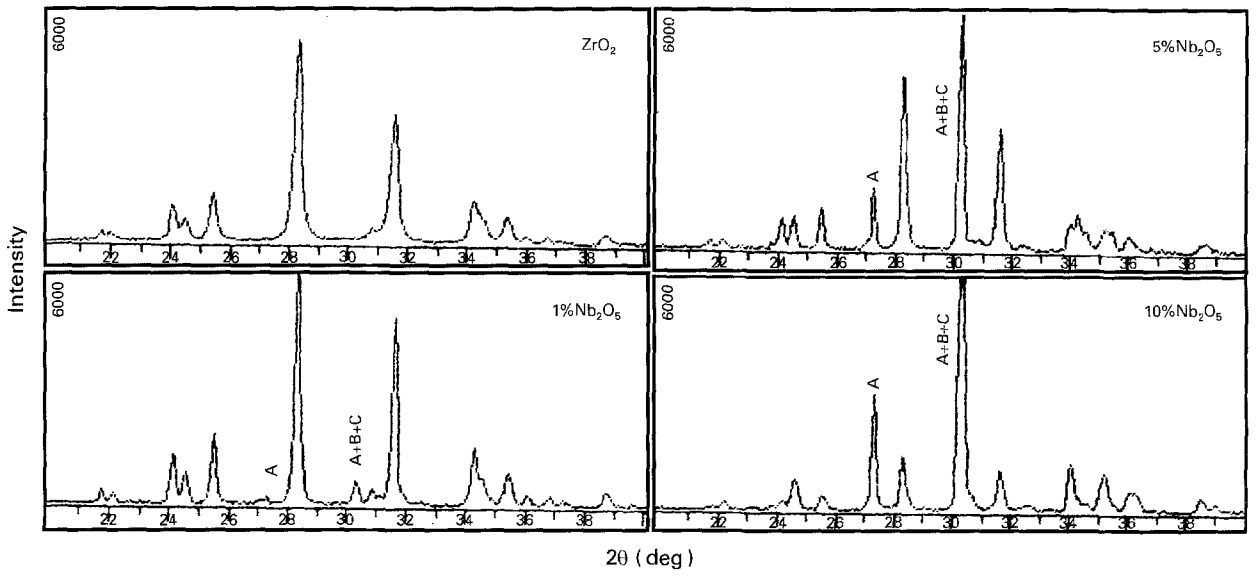

Figure 6 X-ray diffraction patterns of monoclinic ZrO_2 powder and the samples with 1% Nb_2O_5, 5% Nb_2O_5 and 10% Nb_2O_5. It is noted that with the increase of Nb_2O_5 composition, a diffraction peak at around $2\theta = 30.2°$ develops and becomes the strongest peak at $\sim 5\%$ Nb_2O_5; that peak is identified as compounds $Nb_2O_5 \cdot 6ZrO_2$ and $Nb_2O_5 \cdot 8ZrO_2$ plus tetragonal ZrO_2, as indicated in the figure. A, $Nb_2O_5 \cdot 8ZrO_2$; B, $Nb_2O_5 \cdot 6ZrO_2$; C, tetragonal ZrO_2. There is another peak at $\sim 2\theta = 27.3°$, which is identified as $Nb_2O_5 \cdot 8ZrO_2$.

oxidizing condition. Because in α-Zr, zirconium is the predominant element, and in β-Nb, niobium is the predominant one, it is proposed to calculate the Gibbs free energy of ZrO_2 formation in the α-Zr phase and calculate that of Nb_2O_5 in the β-Nb phase. In the 300 °C, $\sim$ 8.6 MPa water oxidizing environment, the oxidation process of zirconium can be divided into two processes:

$$O_2 \rightleftharpoons (\bar{O}_2)_{H_2O} \tag{1}$$

$$\overline{Zr} + (\bar{O}_2)_{H_2O} \rightleftharpoons ZrO_2 \tag{2}$$

where $\overline{Zr}$ indicates zirconium in solid solution. By combining Reactions 1 and 2, we can have the following Reaction 3 as

$$\overline{Zr} + O_2 \rightarrow ZrO_2. \tag{3}$$

So the Gibbs free energy of Reaction 3 is, in fact, the Gibbs free energy of ZrO_2 formation in 300 °C water. According to thermodynamic theory, the Gibbs free energy for Reaction 3 is

$$\Delta G_{ZrO_2} = \Delta G^\circ + RT \ln\left(\frac{1}{\gamma^\alpha_{\overline{Zr}} N^\alpha_{\overline{Zr}} P_{O_2}}\right) \tag{4}$$

where γ^α_{Zr} is the activity coefficient of zirconium in zirconium based α-phase, N^α_{Zr} is the molar fraction of zirconium in that phase and P_{O_2} is the partial pressure of oxygen under the reaction condition (which is 8.6 MPa, i.e. $\sim$86 atm). We assume that the partial pressure of oxygen in 1 atm air is 0.21%, so in $\sim$80 atm, P_{O_2} is $\sim$86 times that in air. In the Zr–Nb phase diagram and referring specifically to the Zr–2.5 wt % Nb alloy at 573 K, we have $\gamma^\alpha_{\overline{Zr}} = 1$, $N^\alpha_{\overline{Zr}} = 0.998$, $P_{O_2} = 18.06$. So we have

$$RT \ln\left(\frac{1}{\gamma^\alpha_{\overline{Zr}} N^\alpha_{\overline{Zr}} P_{O_2}}\right) = -3131.62 \text{ cal mol}^{-1} \tag{5}$$

Because

$$\Delta G^\circ = \Delta H^\circ - T\Delta S^\circ \tag{6}$$

from the *Handbook of Chemistry and Physics* [8], the enthalpy, ΔH°, and entropy, S°, for Reaction 3 are $\Delta H^\circ = -263.1 \text{ kcal mol}^{-1}$, $S^\circ_{ZrO_2} = 12.12 \text{ cal mol}^{-1}\text{K}^{-1}$, $S^\circ_{Zr} = 9.32 \text{ cal mol}^{-1}\text{K}^{-1}$, $S^\circ_{O_2} = 49.0 \text{ cal mol}^{-1}\text{K}^{-1}$. So

$$\Delta S^\circ = S^\circ_{ZrO_2} - S^\circ_{Zr} - S^\circ_{O_2} = -46.2 \text{ cal mol}^{-1}\text{K}^{-1} \tag{7}$$

At 573 K

$$\Delta G^\circ = \Delta H^\circ - T\Delta S^\circ = -236.627 \text{ kcal mol}^{-1} \tag{8}$$

So, the Gibbs free energy for Reaction 3 at 573 K is $\Delta G_{ZrO_2} = -239.759 \text{ kcal mol}^{-1}$.

In the same oxidizing environment

$$\frac{5}{2} O_2 \rightleftharpoons \frac{5}{2} (\bar{O}_2)_{H_2O} \tag{9}$$

$$\overline{Nb} + \frac{5}{2} (\bar{O}_2)_{H_2O} \rightleftharpoons Nb_2O_5 \tag{10}$$

Also, by combining Reactions 9 and 10, we get

$$2\overline{Nb} + \frac{5}{2} O_2 \rightarrow Nb_2O_5 \tag{11}$$

The Gibbs free energy for Reaction 11 is

$$\Delta G_{Nb_2O_5} = \Delta G^\circ + RT \ln\left[\frac{1}{(\gamma^\beta_{\overline{Nb}})^2 (N^\beta_{\overline{Nb}})^2 (P_{O_2})^{5/2}}\right]$$

where $\gamma^\beta_{\overline{Nb}}$ is the activity coefficient of niobium in the niobium-based β-Nb phase and N^β_{Nb} is the molar fraction of niobium in that phase. Because $\Delta G^\circ = \Delta H^\circ - T\Delta S^\circ$ (Equation 6) we also get ΔH° and S° for Reaction 11 as $\Delta H^\circ = -454.0 \text{ kcal mol}^{-1}$,

$S^{\circ}_{Nb_2O_5} = 32.82\ cal\ mol^{-1}\ K^{-1}$, $S^{\circ}_{Nb} = 17.46\ cal\ mol^{-1}\ K^{-1}$. So

$$\Delta G^{\circ} = -454000 + 107.14T\ (cal\ mol^{-1}) \quad (12)$$

Because the β-Nb phase contains ~87% Nb at 573 K, we assume that $\gamma^{\beta}_{Nb} = 1$, $N^{\beta}_{Nb} = 0.87$. So

$$RT \ln \left[\frac{1}{(\gamma^{\beta}_{Nb})^2 (N^{\beta}_{Nb})^2 P_{O_2}{}^{5/2}} \right] = -7891.548\ cal\ mol^{-1}. \quad (13)$$

At 573 K, $\Delta G_{Nb_2O_5} = -400.5\ kcal\ mol^{-1}$. Thus it is concluded that at 573 K, which is the reactor operating temperature, $|\Delta G_{Nb_2O_5}| > |\Delta G_{ZrO_2}|$. This indicates that in aqueous conditions, both Reactions 3 and 11 could occur and the driving force for Reaction 11, i.e. Nb_2O_5 formation, is greater than for Reaction 3 i.e. ZrO_2 formation. Thus both Nb_2O_5 and ZrO_2 would be formed in the β-Nb phase and α-Zr phase respectively during the corrosion of a two-phase Zr–2.5 wt % Nb alloy.

Turning now to our own X-ray diffraction results, Table II and Figs 5 and 6, it is found that $Nb_2O_5 \cdot 6ZrO_2$ and $Nb_2O_5 \cdot 8ZrO_2$ were observed, although some of the reflections were overlapping and interfered with those of ZrO_2 powder, especially the tetragonal ZrO_2. It is well documented [9, 10] that there are three forms of ZrO_2: cubic ZrO_2 is stable only above 1490 °C; tetragonal ZrO_2 is stable between ~1000 and 1490 °C; while monoclinic ZrO_2 is stable at room temperature. By heat treatment of monoclinic ZrO_2 powder to temperatures as high as 1300 °C for 24 h, an allotropic change could occur and the monoclinic ZrO_2 would transform to tetagonal ZrO_2. After furnace cooling, some tetragonal ZrO_2 could be retained and thus be identified by X-ray diffraction. It is also noted that the strongest reflection, (1 1 1), for tetragonal ZrO_2 is also the same strongest reflection for both $Nb_2O_5 \cdot 6ZrO_2$ and $Nb_2O_5 \cdot 8ZrO_2$. There were also some other similar reflections, as can be seen in Table II. The tetragonal ZrO_2 has a lattice parameter of $a = 0.512$ nm, $c = 0.525$ nm; while the orthorhombic $Nb_2O_5 \cdot 6ZrO_2$ is of $a = 0.496$ nm, $b = 0.512$ nm and $c = 0.528$ nm, and orthorhombic $Nb_2O_5 \cdot 8ZrO_2$ is of $a = 0.5283$ nm, $b = 0.5118$ nm and $c = 0.4984$ nm.

Zirconium alloy corrosion is often considered in terms of the effects of a "barrier layer" at the metal–oxide interface which significantly reduces hydrogen ingress and decreases oxidation rates with time, so long as that barrier layer remains intact and protective. TEM work [11] has shown that the oxide at the oxide–metal interface was tetragonal ZrO_2 rather than monoclinic ZrO_2. In the early stages of corrosion (pretransition), the oxide formed on the metal surface is produced mainly from the oxidation of the grain-boundary phases, i.e. β-Zr and its decompositions products. Our own work [12] has demonstrated that Nb_2O_5 is formed during oxidation on β-Nb phase. The incorporation of an element such as niobium into the oxide or "barrier layer" could be possible due to the preferential oxidation of the β-phase in the initial stages of the corrosion process. In fact, it is believed that the poor resistance to oxidation in oxygen-contaminated steam is a result of the preferential attack of a finely distributed niobium-rich phase leading to the localized formation of Nb_2O_5, which subsequently disrupts the adjacent protective oxide [13]. However, a direct relation between niobium in solid solution and the formation of barrier layers has not yet been demonstrated. From the present X-ray diffraction study, it is possible that niobium is incorporated into the oxide by the formation that could be in terms of compounds such as $Nb_2O_5 \cdot 6ZrO_2$ and $Nb_2O_5 \cdot 8ZrO_2$.

As mentioned in Section 1, the compounds formed at the ZrO_2-rich region have a superstructure and could be termed as a continuous homologous series $[(Nb, Zr)_nO_{2n+1}]$, where n varies from ~7–10. The superstructure occurs only in the direction with a multiple cell varying from ~7–10 times the ~5 A cell of the basic fluorite structure [7]. Obviously, the compounds formed ($Nb_2O_5 \cdot 6ZrO_2$ and $Nb_2O_5 \cdot 8ZrO_2$) in the present study were well fitted in the homogeneous series, and could also be written as $(Zr, Nb)_8O_{17}$ and $(Zr, Nb)_{10}O_{21}$. Allpress and Roth [14], by combined X-ray diffraction and electron optical techniques, found the compound to exist in three polymorphs. More detailed examination about the superstructure could be found in Caly's work [15], from which the electron diffraction patterns indicate that the unit cell of any individual crystal of intermediate composition can be exceedingly large.

4. Conclusions

By mixing ZrO_2 and Nb_2O_5 in differing ratios, and heating at 1300 °C for 24 h, two new phases $Nb_2O_5 \cdot 6ZrO_2$ and $Nb_2O_5 \cdot 8ZrO_2$ (or $(Zr, Nb)_8O_{17}$ and $(Zr, Nb)_{10}O_{21}$) were observed from X-ray diffraction patterns. It is noted that some of the reflection peaks of the two compounds are overlapping and interfered with those of the zirconium oxide, especially the tetragonal ZrO_2. It is suggested that the incorporation of niobium into the oxide during the corrosion of Zr–Nb alloys could be by the formation of compounds such as $(Zr, Nb)_8O_{17}$ and $(Zr, Nb)_{10}O_{21}$. Also, the tetragonal ZrO_2 which has been found as a barrier layer oxide, could be, in fact (or partially), the ternary compound $Nb_2O_5 \cdot 6ZrO_2$ and $Nb_2O_5 \cdot 8ZrO_2$ which are orthorhombic with lattice parameters very close to those of the tetragonal ZrO_2.

Acknowledgements

This study was funded by the National Science and Engineering Research Council of Canada through a Research Grant (A4391) awarded to Professor D.O. Northwood. Mr John W. Robinson assisted with the X-ray diffraction analysis. The authors also thank Dr W. V. Youdelis for his suggestions and guidance in the thermodynamic analysis of ZrO_2 and Nb_2O_5 formation.

References

1. C. E. ELLS, S. B. DALGAARD, W. EVANS and W. R. THOMAS, in "Proceedings of the 3rd International Conference on Peaceful Uses of Atomic Energy", Vol. 9 (United Nations, New York, 1964) p. 91.
2. S. A. ALDRIDGE and B. A. CHEADLE, *J. Nucl. Mater.* **42** (1972) 32.
3. D. O. NORTHWOOD and W. L. FONG, *Metallography* **13** (1980) 79.
4. M. K. ASUNDI, S. P. GARY, P. MUKHOPADHYAY, G. P. TIWARI and A. SAROJA, *J. Alloy Phase Diagr.* **2** (1986) 141.
5. R. S. ROTH and L. W. COUGHANOUR, *J. Res. Nat. Bur. Stand.* **NBS55** (1955) 209.
6. H. J. COLDSCHMISIDT, *Metallurgia* **62** (1960) 217.
7. R. S. ROTH, J. L. WARING, W. S. BROWER and H. S. PARKER, "Solid state chemistry", Proceedings of the 5th Mathematical Research Symposium NBS Special Publication 364 (National Bureau Standards, Washington, 1972) p. 183.
8. R. C. WEAST, in "Handbook of chemistry and physics", edited by D. R. Lide, 75th Edn (CRC Press, Boca Raton, FL, 1994).
9. E. GEBHARDT, H. D. SEGHEZZI and W. DUERRSCHNABEL, *J. Nucl. Mater.* **4** (1961) 255.
10. P. EVANS and G. WILDSMITH, *Nature* **189** (1961) 569.
11. Y. DING and D. O. NORTHWOOD, *J. Mater. Sci.* **27** (1992) 1045.
12. F. WANG and D. O. NORTHWOOD, unpublished results (1995).
13. J. K. DAWSON, R. C. ASHER, B. WATKINS, J. BOULTON and J. N. WANKLYN, in "Proceedings of the 3rd International Conference of Peaceful Uses of Atomic Energy", Geneva Vol. 9 (United Nations, New York, 1964) p. 461.
14. J. G. ALLPRESS and R. S. ROTH, *J. Solid State Chem.* **2** (1970) 366.
15. J. CALY, *ibid.* **7** (1973) 277.

Received 1 December 1994
and accepted 15 March 1995